ELSEVIER

Journal of Organometallic Chemistry 650 (2002) 96–107

Journal of Organometallic Chemistry

www.elsevier.com/locate/jorganchem

Preparation, structures, and haptotropic rearrangement of novel dinuclear ruthenium complexes, (μ_2,η^3:η^5-guaiazulene)$Ru_2(CO)_4$(CNR)

Kouki Matsubara [a,c], Shoji Mima [b], Takashi Oda [b], Hideo Nagashima [a,b,c,*]

[a] *Institute of Advanced Material Study, Kyushu University, Kasuga, Fukuoka 816-8580, Japan*
[b] *Interdisciplinary Graduate School of Engineering Sciences, Kyushu University, Kasuga, Fukuoka 816-8580, Japan*
[c] *CREST, Japan Science and Technology Corporation (JST), Kyushu University, Kasuga, Fukuoka 816-8580, Japan*

Received 16 July 2001; received in revised form 10 December 2001; accepted 28 December 2001

Abstract

Novel isonitrile derivatives of a diruthenium carbonyl complex, (μ_2,η^3:η^5-guaiazulene)$Ru_2(CO)_5$ (**2**), were synthesized by substitution of a CO ligand by an isonitrile, and were subjected to studies on thermal and photochemical haptotropic interconversion. Treatment of **2** (a 45:55 mixture of two haptotropic isomers, **2-A** and **2-B**) with RNC at room temperature resulted in coordination of RNC and alternation of the coordination mode of the guaiazulene ligand to form (μ_2,η^1:η^5-guaiazulene)$Ru_2(CO)_5$(CNR), **5d**–**5f**, [**5d**; R = ^{t}Bu, **5e**; 2,4,6-$Me_3C_6H_2$, or **5f**; 2,6-$^i Pr_2C_6H_3$] in moderate to good yields. Thermal dissociation of a CO ligand from **5** at 60 °C resulted in quantitative formation of a desirable isonitrile analogue of **2**, (μ_2,η^3:η^5-guaiazulene)$Ru_2(CO)_4$(CNR), **4d**–**4f**, [**4d**; R = ^{t}Bu, **4e**; 2,4,6-$Me_3C_6H_2$, or **4f**; 2,6-$^i Pr_2C_6H_3$], as a 1:1 mixture of the two haptotropic isomers. A direct synthetic route from **2** to **4d**–**4f** was alternatively discovered; treatment of **2** with one equivalent of RNC at 60 °C gave **4d**–**4f** in moderate yields. All of the new compounds were characterized by spectroscopy, and structures of **5d** (R = ^{t}Bu) and **4d-A** (R = ^{t}Bu) were determined by crystallography. Thermal and photochemical interconversion between the two haptotropic isomers of **4d**–**4f** revealed that the isomer ratios in the thermal equilibrium and in the photostatic state were in the range of 48:52–54:46. © 2002 Elsevier Science B.V. All rights reserved.

Keywords: Isonitrile complexes; Ruthenium complexes; Haptotropic rearrangement; Guaiazulene

1. Introduction

Migration of a transition metal fragment from one coordination site to the other on a π-conjugated polyene or polyaromatic ligand is known as the haptotropic rearrangement [1–3]. Although a number of studies have been made on the haptotropic rearrangement of mononuclear complexes, only a few reports on the rearrangement of dinuclear systems have been published [4]. In our recent studies on the haptotropic rearrangement of dinuclear carbonyl complexes bearing acenaphthylene or guaiazulene ligands [5], we discovered the photochemical and thermal interconversion between two isomers of (μ_2,η^3:η^5-guaiazulene)$Fe_2(CO)_5$ (**1**) (Scheme 1, Eq. (1)) [5a], in which the ratio of the two isomers, **1-A** and **1-B**, in the photostatic state was 35:65, whereas that in the thermal equilibrium was 55:45. The ruthenium homologue of **1**, (μ_2,η^3:η^5-guaiazulene)$Ru_2(CO)_5$ (**2**) was also synthesized; the ratio between the two isomers, **2-A** and **2-B**, was 45:55 both in the photostatic state and in the thermal equilibrium (Scheme 1, Eq. (1)) [5a].

In our further studies on the thermally reversible photoisomerization of **1**, **2**, and their derivatives, we synthesized a series of phosphine and phosphite derivatives of **1** and **2**, (μ_2,η^3:η^5-guaiazulene)$Fe_2(CO)_4$(L) (**3**) [L = PMe_3, PEt_3, $PMePh_2$, PPh_3, P(*p*-Tol)$_3$, PCy_3, P{$(OCH_2)_3CMe$}, and $P(OPh)_3$] and (μ_2,η^3:η^5-guaiazulene)$Ru_2(CO)_4$(L), **4a**–**4c** [**4a**; L = PMe_3, **4b**; P{$(OCH_2)_3CCH_3$}$_3$ **4c**; $P(OPh)_3$]. Although almost all of these derivatives were inactive towards haptotropic isomerization either thermally or photochemically, one particular compound where L = P{$(OCH_2)_3CCH_3$} un-

* Corresponding author. Fax: +81-92-5837819.
E-mail address: nagasima@cm.kyushu-u.ac.jp (H. Nagashima).

0022-328X/02/$ - see front matter
PII: S0022-328X(02)01187-7

derwent the isomerization to give a mixture of **4b-A** and **4b-B** in the thermal equilibrium (**4b-A**:**4b-B** = 100:0) and in the photostatic state (**4b-A**:**4b-B** = 70:30) (Scheme 1, Eq. (3)) [5c]. These results suggest that the *ruthenium* complex, which has *a small and less basic* phosphorus ligand undergoes the isomerization [cone angle of P{$(OCH_2)_3CCH_3$} = 101°]. In fact, the diiron homologue, (μ_2,η^3:η^5-guaiazulene)$Fe_2(CO)_4$[P{$(OCH_2)_3CCH_3$}], does not isomerize under similar conditions as shown in Scheme 2 (Eq. (2)). Neither the ruthenium complex bearing a small but basic ligand

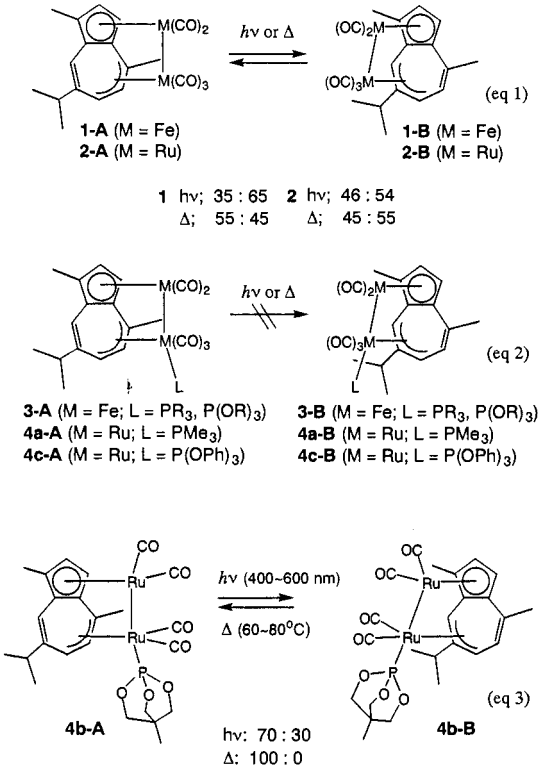

Scheme 1.

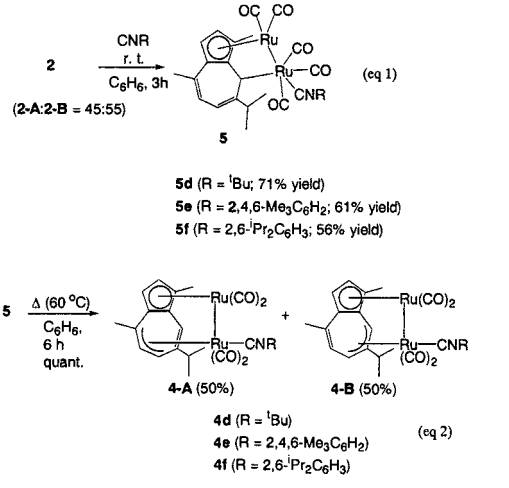

Scheme 2.

(PMe$_3$; cone angle = 118°), (μ_2,η^3:η^5-guaiazulene)Ru_2-$(CO)_4(PMe_3)$ (**4a**), nor that bearing a large and less basic ligand [P(OPh)$_3$: cone angle = 128°], (μ_2,η^3:η^5-guaiazulene)$Ru_2(CO)_4${P(OPh)$_3$} (**4c**), is active towards the thermal or photochemical haptotropic rearrangement. Thus, appropriate choice of a small and less basic ligand other than P{$(OCH_2)_3CCH_3$} as L of (μ_2,η^3:η^5-guaiazulene)$Ru_2(CO)_4$(L) could be a key in the search for a new derivative of **2**, which undergoes the thermally reversible photoisomerization.

In this context, we were interested in isonitriles as one of the small and less basic ligands of (μ_2,η^3:η^5-guaiazulene)$Ru_2(CO)_4$(L); the isonitrile derivatives may undergo the haptotropic isomerization. It is well known that isonitriles are good π-acceptors and moderately strong σ-donors, and are sterically not bulky ligands [6]. Although a synthetic route of the phosphine and phosphite derivatives of (μ_2,η^3:η^5-guaiazulene)Ru_2-$(CO)_4$(L), **4a**–**4c**, via (μ_2,η^1:η^5-guaiazulene)Ru_2-$(CO)_5$(L), **5a**–**5c** [L = PMe$_3$ (**5a**), P(OPh)$_3$ (**5b**), P{$(OCH_2)_3CMe$} (**5c**)], was established as reported earlier [5c], there is no precedence for preparation of their isonitrile homologues, (μ_2,η^3:η^5-guaiazulene)Ru_2-$(CO)_4$(η-CNR) [CNR: R = ^{t}Bu (**4d**), 2,4,6-$Me_3C_6H_2$ (**4e**), 2,6-^{i}Pr$_2$C$_6$H$_3$ (**4f**)], In this paper, we wish to report that **4d**–**4f** were synthesized by a two-step procedure involving addition of CNR to **2** to form (μ_2,η^1:η^5-guaiazulene)$Ru_2(CO)_5$(η-CNR) [CNR: R = ^{t}Bu (**5d**), 2,4,6-$Me_3C_6H_2$ (**5e**), 2,6-^{i}Pr$_2$C$_6$H$_3$ (**5f**)] and subsequent thermal dissociation of a CO ligand in **5d**–**5f**. Alternatively, **4d**–**4f** were prepared by direct reaction of **2** with CNR. The addition of CNR to **2** involves η^3 to η^1 hapticity change of the η^3-allyl moiety of **2**, whereas dissociation of CO from **5d**–**5f** takes place via η^1 to η^3 hapticity change of the η^1-allyl moiety of **5d**–**5f** [7,8]. Studies on thermal and photochemical haptotropic interconversion between two isomers of these new complexes **4d**–**4f** revealed that use of isonitrile ligands as L of (μ_2,η^3:η^5-guaiazulene)$Ru_2(CO)_4$(L) led to successful haptotropic rearrangement as we expected. Comparison in the features of the isomerization with those of **2** and **4b** is also described.

2. Results and discussion

2.1. Stepwise and direct synthetic methods for (μ_2,η^3:η^5-guaiazulene)$Ru_2(CO)_4$(CNR) (4)

As described in our previous paper [5c], phosphine and phosphite substituted complexes (μ_2,η^3:η^5-guaiazulene)$Ru_2(CO)_4$(L), **4a**–**4c**, can be prepared by thermal substitution of a CO ligand in **2** by phosphorus ligands. The preparation involves two elementary reactions, addition of phosphines or phosphites to **2** to form σ-allyl

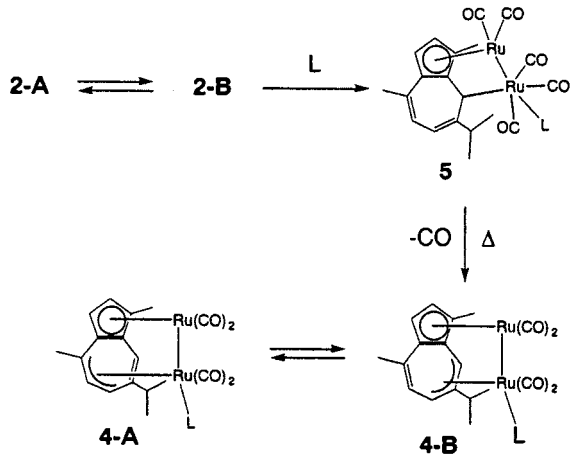

Scheme 3.

complexes ($\mu_2,\eta^1{:}\eta^5$-guaiazulene)$Ru_2(CO)_5$(L), **5a**–**5c**, and subsequent thermal liberation of a CO ligand from ($\mu_2,\eta^3{:}\eta^5$-guaiazulene)$Ru_2(CO)_5$(L), **4a**–**4c** [5c]. The electronic nature of isonitriles is different from either of the phosphorus ligands, which are generally better σ-donors and poorer π-acceptors than isonitriles [6]. Nevertheless, we discovered that addition of RNC to **2** successfully afforded ($\mu_2,\eta^1{:}\eta^5$-guaiazulene)$Ru_2(CO)_5$-(η-CNR) (**5d**–**5f**) [CNR: R = ^{t}Bu (**5d**), 2,4,6-$Me_3C_6H_2$ (**5e**), 2,6-$^i Pr_2C_6H_3$ (**5f**)], and subsequent thermolysis of **5d**–**5f** led to the isonitrile derivatives of **1**, ($\mu_2,\eta^3{:}\eta^5$-guaiazulene)$Ru_2(CO)_5$(η-CNR) (**4d**–**4f**) [CNR: R = ^{t}Bu (**4d**), 2,4,6-$Me_3C_6H_2$ (**4e**), 2,6-$^i Pr_2C_6H_3$ (**4f**)].

In a typical example, the reaction of **2** (a 45:55 mixture of two haptotropic isomers, **2-A** and **2-B**) with *tert*-butylisonitrile at room temperature for 3 h resulted in formation of ($\mu_2,\eta^1{:}\eta^5$-guaiazulene)$Ru_2(CO)_5$-(CN^{t}Bu) (**5d**) (88% based on ^{1}H-NMR). A small amount of unreacted **2-A** was recovered (12% based on ^{1}H-NMR). No other by-product was formed in this reaction. Chromatographic separation of the reaction mixture gave **5d** in 71% isolated yield (Scheme 2, eq. 1). The reactions of **2** with other isonitriles (2,4,6-trimethylphenylisonitrile and 2,6-diisopropylphenylisonitrile) also gave the corresponding σ-allyl complexes, **5e** and **5f**, in 62 and 56% isolated yields, respectively. The isonitrile adducts **5d**–**5f** are intermediates to synthesize **4d**–**4f**, and heating of a benzene solution of **5d**–**5f** at 60 °C for 6 h resulted in quantitative formation of **4d**–**4f**, of which the ratios of the haptotropic isomers, **4-A** and **4-B** were 50:50 (Scheme 2, Eq. (2)) [7]. The overall yields of **4d**–**4f** from the mixture of **2-A** and **2-B** were moderate to good (56–71%) in this two-step procedure.

In this addition reaction of isonitriles, a mixture of **2-A** and **2-B** was used as the starting material; however, **5** was obtained as a single product. There was substantial difference in the reaction rate between **2-A** and **2-B**, and **2-B** reacted much faster than **2-A**. NMR observation of the reaction mixture suggested that addition of RNC to **2-B** smoothly took place by way of the η^3 to η^1 conversion of the η^3-allyl ligand in **2-B**. In contrast, the reaction from **2-A** to **5** involves rearrangement of **2-A** to **2-B** and subsequent conversion of **2-B** to **5**. In the reaction from **5** to **4**, a CO ligand was selectively liberated from the metal center, and no generation of **2**, which could be formed by dissociation of CNR on **5**, was observed. Product **4** obtained by the thermal reaction of **5** was a mixture of two isomers, **4-A** and **4-B**. The reaction profiles showed that **4-B** was the initially formed isomer, and then the content of **4-A** gradually increased with a decrease of both **5** and **4-B**. At the final stage of the reaction, the ratio of **4-A** and **4-B** came to equilibrium (vide infra). This suggests that the reaction involves the initial formation of **4-B** followed by isomerization from **4-A** to **4-B**, The overall scheme is illustrated in Scheme 3.

Overall yields of **4d**–**4f** from **2** by the two-step preparative method were 56–71%. As an alternative route to **4d**–**4f**, a direct synthetic method was achieved by treatment of **2** with a slightly excess amount of the isonitriles at 60 °C for 6 h. The complexes **4d**–**4f** were isolated by column chromatography in moderate yields (**4d**, 44%; **4e**, 44%; **4f**, 35%) (Scheme 4). Addition of the isonitrile to the resulting **4d**–**4f** concomitantly occurred to give ($\mu_2,\eta^1{:}\eta^5$-guaiazulene)$Ru_2(CO)_4(CNR)_2$ (**6**) as a byproduct in 6–22% yields. It was confirmed that treatment of **4d** with ^{t}BuNC at 25 °C for 18 h gave **6d** as a

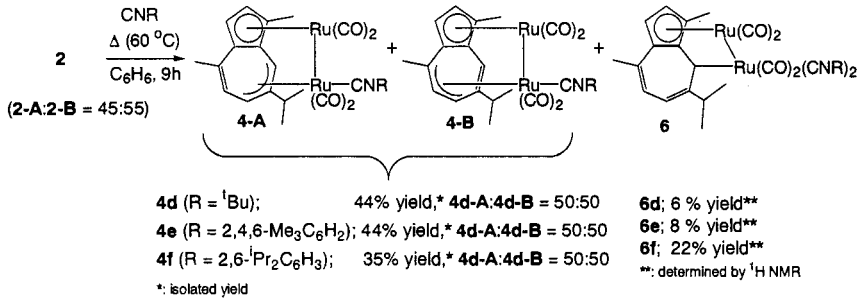

Scheme 4.

Table 1
^{1}H-NMR spectral data for **4d-A**–**4f-A** and **4d-B**–**4f-B**

	4d-A	**4e-A**	**4f-A**
H2	5.26 (d, $J = 3.2$)	5.26 (d, $J = 3.2$)	5.23 (d, $J = 2.8$)
H3	3.28 (d,$J = 3.2$)	3.37 (d, $J = 3.2$)	3.37 (d, $J = 2.8$)
H5	4.88 (d, $J = 8.4$)	5.00 (d, $J = 8.0$)	5.05 (d, $J = 8.4$)
H6	2.92 (d, $J = 8.4$)	3.07 (d, $J = 8.0$)	3.15 (d, $J = 8.4$)
H8	5.07 (s)	5.07 (s)	5.13 (s)
1-Me, 4-Me	1.58, 1.98	1.75, 2.00	1.76, 1.98
CH of ^{i}Pr	1.95 (sep, $J = 6.8$)	2.00 [a]	2.01 (sep, $J = 6.8$)
Me of ^{i}Pr	0.97 (d, $J = 6.8$)	0.95 (d, $J = 6.6$)	0.96 (d, $J = 6.8$)
	0.91 (d, $J = 6.8$)	0.91(d, $J = 6.6$)	0.91 (d, $J = 6.8$)
Others	0.62 (s, 9H, ^{t}Bu)	6.42 (s, 2H, *meta)*	6.94 (t, $J = 8.0$, 1H, *para*)
		2.12 (s, 6H, *ortho*-Me)	6.85 (d, $J = 8.0$, 2H, *meta*)
		1.92 (s, 3H, *para*-Me)	3.37 (br, 1H, Ch of ^{i}Pr)
			1.17 (d, $J = 6.8$, 6H, Me)
			1.16 (d, $J = 6.8$, 6H, Me)
	4d-B	**4e-B**	**4f-B**
H2	5.12 (d, $J = 2.8$)	5.13 (d, $J = 2.4$)	5.10 (d, $J = 2.8$)
H3	5.15 (d, $J = 2.8$)	5.08 (d, $J = 2.4$)	5.06 (d, $J = 2.8$)
H5	4.84 (d, $J = 8.0$)	4.88 (d, $J = 8.4$)	4.91 (d, $J = 8.4$)
H6	3.05 (d, $J = 8.0$)	3.17 (d, $J = 8.4$)	3.29 (d, $J = 8.4$)
H8	4.45 (s)	4.54 (s)	4.57 (s)
1-Me, 4-Me	1.10, 1.26	1.14, 1,28	1.15, 1.27
CH of ^{i}Pr	2.59 (sep, $J = 6.4$)	2.63 (sep, $J = 7.2$)	2.70 (sep, $J = 6.8$)
Me of ^{i}Pr	1.32 (d, $J = 6.4$)	1.31 (d, $J = 7.2$)	1.32 (d, $J = 6.8$)
	1.28 (d, $J = 6.4$)	1.28 (d, $J = 7.2$)	1.30 (d, $J = 6.8$)
Others	0.85 (s, 9H, ^{t}Bu)	6.42 (s, 2H, *meta)*	6.96 (t, $J = 8.0$, 1H, *para)*
		2.17(s, 6H, *ortho*-Me)	6.86 (d, $J = 8.0$, 2H, *meta)*
		1.92(s, 3H, *para*-Me)	3.46 (sep, $J = 6.8$, 1H, CH of ^{i}Pr)
			1.19 (d, $J = 6.8$, 6H, Me)
			1.17 (d, $J = 6.8$, 6H, Me)

Measured in C_6D_6 (δ, ppm; J, Hz). The numbering of protons (H1–H8, 1-Me, and 4-Me) on the guaiazulene ligand is shown below.
[a] Determined by ^{1}H–^{1}H COSY spectrum.

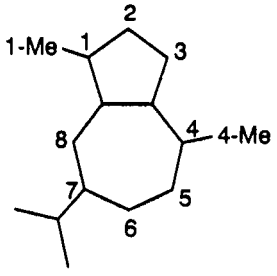

mixture of two isomers due to the arrangement of CO and RNC ligands (83% yield based on ^{1}H-NMR, and 44% isolated yield after recrystallization) [9,10]. It is of interest that no by-product such as (μ_2,η^1:η^5-guaiazulene)$Ru_2(CO)_4(PR_3)_2$ was formed in the reaction of the mixture of **2-A** and **2-B** with phosphines and phosphites [5].

*2.2. Isolation and characterization of (μ_2,η^3:η^5-guaiazulene)$Ru_2(CO)_4$(CNR) (**4**) and (μ_2,η^1:η^5-guaiazulene)$Ru_2(CO)_5$(CNR) (**5**)*

The isonitrile complex **4d**–**4f** was obtained as a mixture of two haptotropic isomers. Separation of the isomers was done by fractional recrystallization from a CH_2Cl_2–hexane solution at -30 °C; **4d-A**, **4e-A**, **4e-B**, and **4f-A** were obtained in analytically pure form. Two other isomers, **4d-B** and **4f-B**, containing a small amount of **4d-A** and **4f-A**, respectively, were characterized by spectroscopic methods. Spectral data for **4d**–**4f** are summarized in Tables 1 and 2. IR absorption due to the CN bond appeared around 2100–2150 cm^{-1}. Four absorption bands assigned to ν_{CO} were also seen (1900–2000 cm^{-1}). Although the ^{13}C resonance due to the CN moiety of the CNR ligand was not observed even at low temperatures, four ^{13}C resonances due to the carbonyl ligands were observed around δ 195–220 at -50 °C; for example, the CO signals of **4d-A** ap-

peared at δ 218.2, 211.7, 207.3, 197.1 in the ^{13}C-NMR. The ^{1}H resonances due to the H5 and H6 protons (H5: δ 4.88–5.05, H6: δ 2.92–3.15) and ^{13}C resonances due to the C4–C6 carbons of **4d-A**, **4e-A** or **4f-A** appeared at higher fields (δ 42–81) than the H8 (δ 5.07–5.13) and the C7–C8 (δ 107–150) resonances, respectively. The upfield shift is due to the bonding interaction between the C4–C6 carbons and the ruthenium atom. In contrast, ^{1}H and ^{13}C resonances due to the H6 and H8 protons and the C6–C8 carbons of the haptotropic isomers **4d-B**, **4e-B** or **4f-B** were visible in higher field than those of the H5 proton and the C4–C5 carbons, respectively, suggesting the coordination of C4–C6 to the ruthenium atom.

Table 2
^{13}C-NMR and IR spectral data for **4d-A**–**4f-A** and **4d-B**–**4f-B**

	4d-A [b]	**4e-A**	**4f-A**
^{13}C [a]; C1	103.7	102.9	103.0
C2	83.8	83.6	83.7
C3	74.3	74.1	74.2
C4	71.8	72.4	72.8
C5	80.9	81.3	79.7
C6	42.4	44.3	44.5
C7	150.0	150.0	148.6
C8	107.4	107.0	107.2
C9	87.5	87.0	87.0
C10	86.5	86.3	86.4
1-Me, 4-Me	13.5, 24.5	12.6, 24.2	12.6, 24.3
CH of ^{i}Pr	39.3	38.3	38.4
Me of ^{i}Pr	23.4, 22.2	22.6,21.6	22.6, 21.6
CO	218.2, 211.7, 207.3, 197.1	210.8, 205.5	not observed
CN	not observed	not observed	not observed
Others	57.5 ($C(CH_3)_3$)	138.0 (*para*)	128.9 (*para*)
	30.4 ($C(CH_3)_3$)	128.7 (*meta*)	123.7 (*meta*)
		134.5 (*ortho*)	30.3 (CH of ^{i}Pr)
		20.9 (*para*-Me)	22.9 (Me)
		18.7 (*ortho*-Me)	22.8 (Me)
IR (KBr, cm^{-1})	2116 (CN)	2122 (CN)	2123 (CN)
	2003 (CO), 1962 (CO)	1985 (CO), 1953 (CO)	2002 (CO), 1964 (CO)
	1907 (CO)	1931 (CO), 1911 (CO)	1947 (CO), 1905 (CO)
	4d-B [b]	**4e-B**	**4f-B**
^{13}C [a]; C1	92.5	92.5	92.5
C2	82.7	82.8	83.0
C3	80.5	80.4	80.5
C4	107.9	107.9	108.0
C5	126.8	126.5	126.4
C6	49.7	49.7	49.9
C7	121.8	121.9	122.0
C8	50.2	50.2	50.3
C9	79.5	79.5	79.5
C10	87.2	87.0	87.2
1-Me, 4-Me	11.0, 20.4	10.7, 20.2	10.7, 20.3
CH of ^{i}Pr	37.9	37.7	37.9
Me of ^{i}Pr	28.0, 18.8	27.9, 18.7	28.0, 18.6
CO	219.2, 211.2, 206.1, 197.0	210.8, 205.5	210.9, 205.6
CN	not observed	not observed	not observed
Others	57.3 ($C(CH_3)_3$)	138.0 (*para*)	128.9 (*para*)
	30.1 ($C(CH_3)_3$)	128.7 (*meta*)	123.7 (*meta*)
		134.3 (*ortho*)	30.3(Ch of ^{i}Pr)
		20.9 (*para*-Me)	23.0 (Me)
		18.6 (*ortho*-Me)	22.9 (Me)
IR (KBr, cm^{-1})	2151 (CN)	2099 (CN)	2114 (CN)
	1984 (CO), 1949 (CO)	2002 (CO), 1952 (CO)	1999 (CO), 1958 (CO)
	1913 (CO)	1904 (CO)	1940 (CO), 1906 (CO)

[a] Measured in C_6D_6 (δ, ppm; J, Hz). The numbering of carbons (C1–C8, 1-Me, and 4-Me) on the guaiazulene ligand is shown in Table 1.
[b] ^{13}C-NMR spectra were measured at -50 °C.

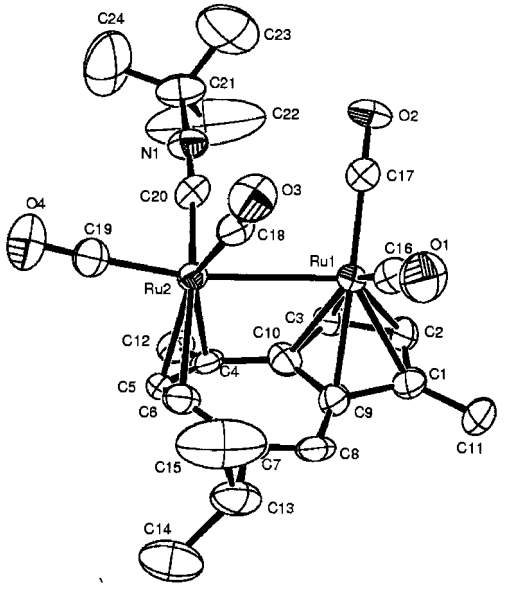

Fig. 1. ORTEP drawing of **4d-A**. 50% probability of thermal ellipsoids.

Table 3
Representative bond lengths (Å) and angles (°) of **4d-A**

Bond lengths			
Ru(1)–Ru(2)	2.8728(8)	Ru(1)–C(16)	1.86(1)
Ru(1)–C(1)	2.261(7)	Ru(1)–C(17)	1.882(9)
Ru(1)–C(2)	2.249(8)	Ru(2)–C(18)	1.889(8)
Ru(1)–C(3)	2.234(8)	Ru(2)–C(19)	1.848(8)
Ru(1)–C(9)	2.227(7)	C(10)–C(4)	1.44(1)
Ru(1)–C(10)	2.261(7)	C(4)–C(5)	1.38(1)
Ru(2)–C(4)	2.331(7)	C(5)–C(6)	1.43(1)
Ru(2)–C(5)	2.179(6)	C(6)–C(7)	1.47(1)
Ru(2)–C(6)	2.252(7)	C(7)–C(8)	1.33(1)
Ru(2)–C(20)	1.988 (8)	C(8)–C(9)	1.46(1)
Bond angles			
Ru(2)–Ru(1)–C(16)	101.5(3)	C(18)–Ru(2)–C(20)	99.9(3)
Ru(2)–Ru(1)–C(17)	97.2(3)	Ru(1)–C(20)–N(1)	175.8(7)
Ru(1)–Ru(2)–C(18)	73.6(2)	Ru(1) –C(16)–0(1)	175(1)
Ru(1)–Ru(2)–C(19)	167.5(2)	Ru(1)–C(17)–O(2)	178(1)
Ru(1)–Ru(2)–C(20)	85.6(2)	Ru(2)–C(18)–O(3)	173(1)
C(16)–Ru(1) –C(17)	91.7(4)	Ru(2)–C(19)–0(4)	178(1)
C(18)–Ru(2)–C(19)	95.2(3)	C(20)–N(1)–C(21)	176.2(8)
C(19)–Ru(2)–C(20)	91.0(3)		

The molecular structure of **4d-A** determined by a single crystal X-ray diffraction study is in good agreement with the spectroscopic data (Fig. 1). The structure of **4d-A** is similar to that of the phosphite derivative **4b-A** [5c]. Representative bond lengths and angles of **4d-A** are listed in Table 3. The C(1)–C(3) and C(9)–C(10) of the guaiazulene ligand are bound to the Ru(1) atom, whereas C(4)–C(6) carbons bond with the Ru(2) atom. Thus, the coordination mode of the guaiazulene ligand is $\mu_2,\eta^3{:}\eta^5$. The Ru(2)–C(4), Ru(2)–C(5), and Ru(2)–C(6) bond distances are 2.18–2.33 Å, which are similar to those in **2-A** (2.20–2.34 Å) or **4b-A** (2.19–2.31 Å). The metal–metal bond distance (Ru–Ru) is 2.8728(8) Å [cf. **2-A** (2.8795(5) Å) and **4b-A** (2.873(1) Å)]. The isonitrile ligand is coordinated to the Ru(2) atom with a bond distance of 1.988(8) Å which is in the range of the Ru–C(isonitrile) distances of known isonitrile complexes of ruthenium (1.9–2.1 Å) [11]. A notable difference in the crystal structure between the phosphite complex **4b-A** and the isonitrile analogue **4d-A** is arrangement of the ligands around Ru(2). In **4b-A**, geometry at the Ru(2) atom can be described as a distorted trigonal bipyramid, in which the phosphite ligand and the Ru(1) atom occupy the apical positions. In contrast, one of the CO ligands and the Ru(1) atom occupy the apical positions, and the isonitrile ligand is located at the equatorial position in **4d-A**. In solution, three possible isomers of **4d-A** derived from the arrangement of the isonitrile ligand were visible. At −70 °C, three sets of ^{1}H resonances due to the guaiazulene ligand and three signals due to the *tert*-butyl group of the isonitrile ligand were observed in a ratio of 77:18:9. Broadening of these signals was observed at −10 to 40 °C. Above 0 °C, NMR spectrum of **4d-A** showed a single set of ^{1}H resonances due to the guaiazulene ligand and the *tert*-butyl group of the isonitrile ligand. Above room temperature, the haptotropic isomerization of **4d-A** to **4d-B** was also observed. Similarly, three isomers were observed in ^{1}H-NMR spectra of **4e-A** and **4e-B** at −70 °C, in which the ratios were 61:32:7 and 58:32:10, respectively. The ^{13}C-NMR data of **4d-A** provided direct evidence for the site exchange process of the CO and isonitrile ligands [12,13]. Existence of three isomers provided three sets of four ^{13}C peaks due to the four CO ligands in the ^{13}C-NMR spectrum below −50 °C, while at −30 °C, only a single set of four sharp signals at δ 197, 206, 211, and 219 was visible. The two peaks at δ 197 and 219 broadened at −20 °C and disappeared at −10 °C. At −10 °C, the other two signals broadened. These NMR data suggest that the site exchange of two CO and one isonitrile ligand in **4d**–**4f** occurs quickly in solution [12,13]. In other words, there is little difference in energy among three possible isomers due to the arrangement of two CO and one isonitrile ligand around the Ru(2) atom, though only one isomer of **4d-A** was visible in the crystal structure.

The σ-allyl intermediates **5d**, **5e**, and **5f** were characterized by spectroscopy (Table 4). The ^{13}C resonances due to the CN moiety of **5d**–**5f** appeared at δ 159.7–160.0, whereas ν_{C-N} absorption appeared at 2185 (**5d**), 2153 (**5e**), or 2160 (**5f**) cm^{-1}. The existence of the five CO ligands of **5d**–**5f** was revealed by observation of five signals at δ 192–211 in the ^{13}C-NMR and five IR absorptions at 1900–2059 cm^{-1}. Their ^{1}H- and ^{13}C-NMR spectra showed that the proton assignable to H8 and the carbon due to C8 appeared at unusually high-field regions (δ 2.82–3.14 in ^{1}H-NMR, δ 14.3–18.0 in ^{13}C-NMR); characteristic upfield shift of the signals due

Table 4
Spectral data for **5d**–**5f**

	5d	**5e**	**5f**
^{1}H			
H2	5.26 (d, $J = 2.0$)	5.15 (d, $J = 6.6$)	5.14 (brs)
H3	4.98 (d, $J = 2.0$)	4.93 (d, $J = 6,6$)	4.91 (brs)
H5	5.56 (d, $J = 8.0$)	5.59 (d, $J = 7.2$)	5.58 (d, $J = 7.2$)
H6	5.21 (d, $J = 8.0$)	5.25 (d, $J = 7.2$)	5.23 (d, $J = 7.2$)
H8	2.95 (s)	2.82 (s)	3.14 (s)
1-Me	1.15	1.08	1.13
4-Me	1.69	1.70	1.68
CH of ^{i}Pr	2.75 (sep, $J = 7$)	2.40 (sep, $J = 6$)	2.82 (sep, $J = 6$)
Me of ^{i}Pr	1.33 (d, $J = 7$)	1.38 (d, $J = 6.0$)	1.38 (d, $J = 6.0$)
^{i}Pr	1.26 (d, $J = 7$)	1.29 (d, $J = 6.0$)	1.29 (d, $J = 6.0$)
Others	0.71	6.29 (s, 2H, *meta*)	6.77 (d, *meta*)
	(s, 9H, ^{t}Bu)	2.09	6.90 (t, *para*)
		(s, 6H, *ortho*-Me)	3.37 (sep, $J = 6.6$, CH)
		1.82	1.13 (d, $J = 6.$ 6, Me)
		(s, 3H, *para*-Me)	l.13(d, $J = 6.6$, Me)
^{13}C(^{1}H}			
C2	86.2	86.1	86.2
C3	80.0	79.6	79.6
C5	129.9	129.5	129.5
C6	112.3	112.2	112.1
C8	17.8	14.3	18.0
1-Me	11.6	10.8	10.8
4-Me	23.0	22.6	22.8
CH of ^{i}Pr	36.6	36.1	36.0
Me of ^{i}Pr	22.1	21.5	22.6
^{i}Pr	25.2	24.7	24.9
CO	210.9	210.4	209.1
	209.8	209.2	205.8
	206.7	206.0	195.5
	194.0	193.5	193.3
	192.3	191.8	191.5
CN	160.2	159.7	159.7
Others	58.4 ($C(CH_3)_3$)	138.0 (*para*)	145.7 (*ipso*)
	29.8 ($C(CH_3)_3$)	128.7 (*meta*)	130.2 (*para*)
		134.5 (*ortho*)	123.8 (*meta*)
		20.9 (*para*-Me)	30.0 (CH of ^{i}Pr)
		18.4 (*ortho*-Me)	23.0(Me of ^{i}Pr)
IR (KBr, cm^{-1})	2185 (CN)	2153 (CN)	2160 (CN)
	2048 (CO)	2059 (CO)	2049 (CO)
	1992 (CO)	2020 (CO)	2007 (CO)
	1980 (CO)	1978 (CO)	1979 (CO)
	1947 (CO)	1960 (CO)	1959 (CO)
	1901 (CO)	1907 (CO)	1906 (CO)

^{1}H- and ^{13}C-NMR spectra were measured in C_6D_6 at 25 °C (δ, ppm; J, Hz). The numbering of protons and carbons (H1–H8, C1–C8, 1-Me, and 4-Me) on the guaiazulene ligand is shown in Table 1.

to H8 and C8, which was also observed in (μ_2,η^1:η^5-guaiazulene)$Ru_2(CO)_5(PR_3)$ (**5a**–**5c**) (δ 3.14–3.23 in ^{1}H-NMR, δ 15.3–16.1 in ^{13}C-NMR), indicates that the C8 carbon is bonded to the ruthenium atom [5c]. No sign of coordination was observed in other H and C resonances due to protons and carbons of diene moiety in the seven membered ring of the guaiazulene ligand. These results suggest that the structures of **5d**–**5f** are similar to those of **5a**–**5c** [5c]; this is supported by the molecular structure of **5d** shown in Fig. 2. Representative bond lengths and bond angles are listed in Table 5. The crystal structure of **5d** resembles that of the PMe_3 adduct, (μ_2,η^1:η^5-guaiazulene)$Ru_2(CO)_5(PMe_3)$ (**5a**) [5c]. Only the position of the isonitrile ligand in **5d** is different from that of the PMe_3 ligand in **5a**; the PMe_3 located at the *trans* position of the C(8) carbon, whereas the ^{t}BuNC was at the *cis* position of the C(8) carbon. The Ru(2)–C(8) bond length of **5d** is 2.245(3) Å, which is 0.04 Å longer than the Ru(2)–C(8) bond length of the PMe_3 adduct. The Ru(2)–C(21) (CN^tBu) distance is 2.024(3) Å. No scrambling process of the CO and isonitrile ligands was observed in **5d**–**5f** in ^{1}H- and ^{13}C-NMR at room temperature; this implies that the isomer of **5d** shown in the crystal structure, in which the isonitrile ligand is located at the *cis* position of the adjacent ruthenium atom, may be thermodynamically more stable than the other possible isomers [14].

*2.3. Thermal and photochemical haptotropic isomerization of **4a**, **4b**, and **4c***

As described above, we considered that sterically not bulky and electronically less basic ligand (L) is an important factor in the haptotropic isomerization of (μ_2,η^3:η^5-guaiazulene)$Ru_2(CO)_4(L)$, Successful isolation of the haptotropic isomers, **4d-A**, **4e-A**, and **4f-A**, made studies on the thermal and photochemical haptotropic rearrangement of these complexes possible (Scheme 5). Thermal reaction of the separated isomer, **4d-A**, **4e-A**, or **4f-A**, in toluene-d_8 at 60 °C gave an equilibrium mixture of **4-A** and **4-B** (**4d-A**:**4d-B** = 52:48, **4e-A**:**4e-B** = 48:52, **4f-A**:**4f-B** = 50:50) after 15 h (Scheme 5). The isomer ratios of **4d**, **4e**, and **4f** (**4-A**: **4-B** = ca. 50:50) in thermal equilibrium were different from that of **4b** (**4b-A**:**4b-B** = 100:0), and rather similar to that of **2** (**2-A**:**2-B** = 45:55).

Compounds **4d-A**, **4e-A**, and **4f-A** were photoirradiated using a 500 W Xenon lamp through a water filter in toluene-d_8 for 4–13 h. In order to exclude a possibility that the thermal isomerization pathway was involved in the photoisomerization, the reaction was carried out at −20 °C, at which controlled experiments revealed that no thermal rearrangement took place. The photolysis at this temperature yielded a mixture of haptotropic isomers (**4d-A**:**4d-B** = 51:49, **4e-A**:**4e-B** = 50:50, **4f-A**:**4f-B** = 54:46) in the photostatic

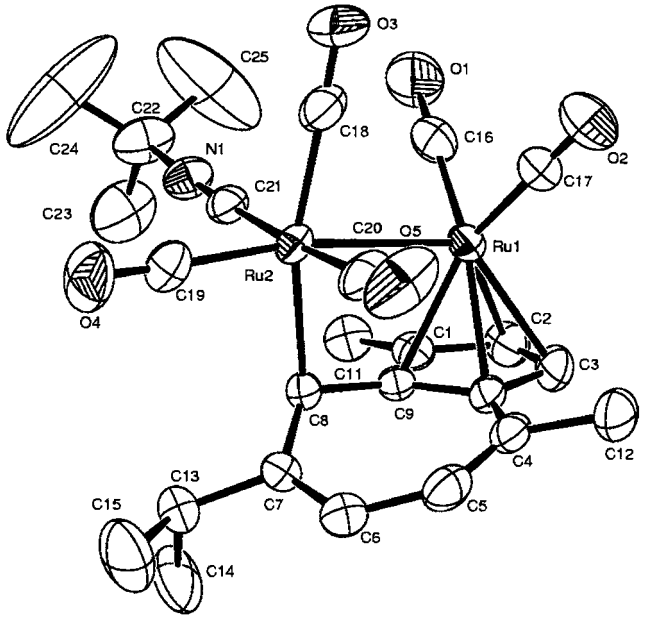

Fig. 2. ORTEP drawing of **5d**. 50% probability of thermal ellipsoids.

Table 5
Representative bond lengths (Å) and angles (°) of **5d**

Bond lengths			
Ru(1)–Ru(2)	2.8095(4)	Ru(2)–C(19)	1.905(3)
Ru(1)–C(1)	2,253(3)	Ru(2)–C(20)	1.939(4)
Ru(1)–C(2)	2.253(3)	Ru(2)–C(21)	2.024(3)
Ru(1)–C(3)	2.243(3)	C(21)–N(1)	1.146(4)
Ru(1)–C(9)	2.268(3)	C(10)–C(4)	1.458(5)
Ru(1)–C(10)	2.252(3)	C(4)–C(5)	1.334(5)
Ru(2)–C(8)	2.245(3)	C(5)–C(6)	1.453(5)
Ru(1)–C(16)	1.860(4)	C(6)–C(7)	1.349(4)
Ru(1)–C(17)	1.859(4)	C(7)–C(8)	1.480(4)
Ru(2)–C(18)	1.932(4)	C(8)–C(9)	1.461(4)
Bond angles			
Ru(2)–Ru(1)–C(16)	97.6(1)	Ru(1)–C(16)–O(1)	178.7(5)
Ru(2)–Ru(1)–C(17)	93.5(1)	Ru(1)–C(17)–O(2)	178.9(4)
Ru(1)–Ru(2)–C(4)	77.63(7)	Ru(2)–C(18)–O(3)	179.1(3)
Ru(1)–Ru(2)–C(18)	83.8(1)	Ru(2)–C(19)–O(4)	177.8(4)
Ru(1)–Ru(2)–C(19)	171.0(1)	Ru(2)–C(20)–O(5)	169.5(3)
Ru(1)–Ru(2)–C(20)	89.0(1)	Ru(2)–C(21)–N(1)	173.7(3)
Ru(1)–Ru(2)–C(21)	91.63(9)	C(21)–N(1)–C(22)	176.3(4)
C(16)–Ru(1)–C(17)	90.2(2)		

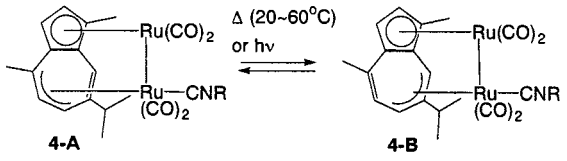

	Δ	hν
	A : B	A : B
4a	52 : 48	51 : 49
4b	48 : 52	50 : 50
4c	50 : 50	54 : 46

Scheme 5.

state. Since the reaction was accompanied by some decomposition of the products (14–20% after 4–13 h, 50–70% after 20 h), exact comparison of the isomer ratios in the photostatic states among **2**, **4b**, and **4d**–**4f** is difficult; however, it is worthwhile to point out that the isomer ratio in the thermal equilibrium or at the photostatic state is similar to that observed in the photoisomerization of **2** rather than that of **4b**. This indicates that the π-acid nature of CO, CNR, and $P(OR)_3$ is an important factor for the successful isomerization between the two isomers of (μ_2,η^3:η^5-guaiazulene)$Ru_2(CO)_4(L)$. In the case of the phosphite derivative **4b**, P{$(OCH_2)_3CMe$} is small but still has substantial steric repulsion towards the methyl and isopropyl groups in the guaiazulene ligand; this resulted in the thermal equilibrium ratio of **4b-A**:**4b-B** = 100:0. At the photo-excited states of **4b-A** and **4b-B**, too, this steric repulsion is important to give a higher ratio of **4b-B** (70:30). In sharp contrast, sterically much smaller CNR does not induce substantial repulsion towards the methyl and isopropyl substituents of the guaiazulene ligand; this provides similar isomer ratios in the thermal equilibrium and at the photostatic state to those of the CO derivative **2**.

3. Conclusion

As described in this paper, stepwise and direct synthetic procedures for isonitrile derivatives of (μ_2,η^3:η^5-guaiazulene)$Ru_2(CO)_5$ (**2**) were established. In particular, the two-step preparative method via **5** gave **4** in moderate to good yields. Isolation of η^1-allyl intermediate **5** indicates that η^3 to η^1 conversion of the η^3-allyl moiety in **2** and η^1 to η^3 hapticity change of the η^1-allyl moiety in **5** play important roles in the synthesis of **4**. The electronic nature of the isonitrile ligands is less π-acidic than CO ligands [6]. In contrast, its steric bulkiness is somewhat larger than CO, but is much smaller than phosphites. The results of the photochemical and thermal haptotropic rearrangement indicate that the π-acidic nature of the isonitrile ligands contributes to successful haptotropic isomerization, but their sterically small structures are not suitable to attain large differences between the photochemical and thermal isomer ratios. In other words, appropriate choice of a π-acidic ligand with appropriate steric bulkiness as L of (μ_2,η^3:η^5-guaiazulene)$Ru_2(CO)_5(L)$ could be a key in the search for a new derivative of **2**, which undergoes the thermally reversible photoisomerization with substantially different isomer ratios between the thermal and photochemical processes. Although suppression of photo-induced decomposition of the isonitrile complexes is a problem to be overcome, the present results suggest that isonitriles with a relatively large alkyl group could be one candidate for L.

4. Experimental

4.1. General procedures

All experiments were carried out in an argon atmosphere using standard Schlenk techniques. THF, benzene, toluene, hexane and benzene-d_6 were distilled from benzophenone ketyl and stored in an argon atmosphere. Other solvents, *tert*-butylisonitrile, and 2,4,6-trimethylphenylisonitrile were used as received. 2,6-diisopropylphenylisonitrile was prepared from 2,6-diisopropylphenylformamide according to a similar procedure reported in organic synthesis [15]. NMR spectra were taken with a JEOL Lambda 400 or 600 spectrometer. Chemical shifts were recorded in ppm using the solvent signals as internal standards. IR spectra (KBr) were taken with a JASCO FT/IR-550 spectrometer using KBr tablets and recorded in cm^{-1}. The ruthenium complex **1** was prepared according to the published method [4a]. Photolysis of **4d**–**4f** was carried out with an Ushio 500 W Xenon lamp through a water filter.

4.2. Synthesis

4.2.1. General synthetic methods ($\mu_2,\eta^1{:}\eta^5$-guaiazulene)$Ru_2(CO)_5$(CNR) (5)

In a typical example, a mixture of **2-A** and **2-B** (45:55, 102 mg, 0.185 mmol) was dissolved in benzene (20 ml) in a 50 ml Schlenk tube. Then, *tert*-butylisocyanide (63 μl, 0.56 mmol) was added and the solution was stirred for 3 h at room temperature (r.t.). The NMR spectrum of the crude mixture revealed the formation of **5d** (88%) with a recovery of **2-A** (12%), After removal of the solvent in vacuo, the residue containing **5d** and **2-A** was subjected to chromatographic separation (Al_2O_3). Elution by hexane–CH_2Cl_2 (20:1) first gave a yellow band containing **2-A** (7.5 mg, 0.014 mmol, 7%). A red–brown band containing **5d** was then obtained by eluting with hexane–CH_2Cl_2 (3:1) (82.0 mg, 0,131 mmol, 71%). Compounds **5e** and **5f** were also given in the same manner as above. Yields of **5e** and **5f** were 62 and 56%, respectively. Spectral data for **5d**–**5f** are shown in Table 4.

5d: Orange crystals; m.p. 114 °C (dec.). Anal. Calc. for $C_{25}H_{27}NO_5Ru_2$: C, 48.15; H, 4.36; N, 2.25. Found: C, 48.29; H, 4.37; N, 2.30%. **5e**: Orange crystals; m.p. 99 °C (dec.). Anal. Calc. for $C_{30}H_{29}NO_5Ru_2$: C, 52.55; H, 4.26; N, 2.04. Found: C, 53.18; H, 4,24; N, 2.04%. **5f**: Orange crystals; m.p. 116.5 °C (dec.). Anal. Calc. for $C_{32}H_{33}NO_4Ru_2$: C, 54.46; H, 4.85; N, 1.92. Found: C, 54.59; H, 4.88; N, 1.94%.

4.2.2. Synthesis of ($\mu_2,\eta^3{:}\eta^5$-guaiazulene)$Ru_2(CO)_4$(CNR) (4)

In a typical example, **5d** (60.0 mg, 0.096 mmol) was dissolved in benzene (20 ml) in a 50 ml Schlenk tube. The solution was heated at 60 °C for 6 h. After removal of the solvent in vacuo, a mixture of **4d-A** and **4d-B** (50:50) was obtained as yellow solids in quantitative yields from **5d** (41 mg, 0.068 mmol, 71% yield from **1**). Using a similar procedure, **4e** or **4f** was also quantitatively obtainable as a 1:1 mixture of **4e-A** and **4e-B** or **4f-A** and **4f-B**. Fractional recrystallization from a mixture of CH_2C1_2 and hexane at −30 °C made separation of the haptotropic isomers possible, and analytically pure samples of **4d-A**, **4e-A**, and **4f-A** were obtained. Complete purification of the isomers, **4d-B**, **4e-B**, and **4f-B**, was unsuccessful; however, they were identified by spectroscopic data. Spectral data for **4d**–**4f** are summarized in Tables 1 and 2.

4d-A; Yellow crystals; m.p. 158 °C (dec.). Anal. Calc. for $C_{24}H_{27}NO_4Ru_2$: C, 48.40; H, 4.57; N, 2.35. Found: C, 48.29; H, 4.58; N, 2.32%. **4e-A**: Yellow crystals; m.p. 121 °C (dec.). Anal. Calc. for $C_{24}H_{27}NO_4Ru_2$: C, 52.96; H, 4.44; N, 2.13. Found: C, 52.70; H, 4.52; N, 2.11%. **4f-A**: Yellow crystals; m.p. 98 °C (dec.). Anal. Calc. for $C_{24}H_{27}NO_4Ru_2$: C, 54.93; H, 5.04; N, 2.00. Found: C, 54.98; H, 5.16; N, 1.99%.

4.2.3. Alternative synthetic methods of" ($\mu_2,\eta^3{:}\eta^5$-guaiazulene)$Ru_2(CO)_4$(CNR) (4)

In a typical example, a mixture of **2-A** and **2-B** (45:55, 50.7 mg, 0.094 mmol) was dissolved in benzene (15 ml) in a 50 ml Schlenk tube. *tert*-Butylisonitrile (12.5 μl, 0.111 mmol) was added and the mixture was stirred at 60 °C for 6 h. After removal of the solvent in vacuo, the residue was purified by column chromatography (Al_2O_3). Elution with hexane–CH_2Cl_2 (20:1) first gave a yellow band containing **2-A** (10.9 mg, 0.020 mmol, 22%). The second yellow band containing **4d-A** and **4d-B** was then obtained by eluting with hexane–CH_2Cl_2 (5:1) (25 mg, 0.041 mmol, 44%). Using similar methods, **4e** and **4f** were obtained in 44 and 35% yields, respectively. Addition of the isonitrile to the resulting **4d**–**4f** concomitantly occurred in these reactions to give ($\mu_2,\eta^1{:}\eta^5$-guaiazulene)$Ru_2(CO)_4(CNR)_2$ (**6**) as a by-product. The yields of **6d** (L = CN^{t}Bu), **6e** (L = CN-2,4,6-$Me_3C_6H_2$), and **6f** (L = CN-2,6-$^i Pr_2C_6H_3$) determined by ^{1}H-NMR spectra of the crude mixtures were 6, 8, and 22%, respectively.

4.2.4. Synthesis of ($\mu_2,\eta^1{:}\eta^5$-guaiazulene)$Ru_2(CO)_4(CN^tBu)_2$ (6d)

The compound **4d** (90.8 mg, 0.152 mmol) was dissolved in benzene (25 ml) in a 50 ml Schlenk tube; *tert*-butylisonitrile (68.3 μl, 0.608 mmol) was added and the mixture was stirred at 25 °C for 18 h. After removal of the solvent in vacuo, the residue was extracted with heptane. Crystals of **6d** containing a small amount of **4d** were obtained by cooling the solution at −30 °C (45 mg, 0.067 mmol, 44% yield). Analytically pure

samples were obtained by fractional recrystallization of the crude product from CH_2C1_2 and hexane. The compound **6d** was a mixture of two isomers (60:40). Orange crystals; m.p. 128 °C (dec.). Anal. Calc. for $C_{29}H_{36}N_2O_4Ru_2$: C, 51.32; H, 5.35; N, 4.13. Found: C, 51.01; H, 5.34; N, 4.01%. IR (KBr, cm^{-1}): 2182 (CN), 2156 (CN), 2006 (CO), 1961 (CO), 1943 (CO), 1947 (CO), 1889 (CO).

Major isomer: ^{1}H-NMR(C_6D_6, rt): δ 5.69 (d, J_{HH} = 7.2 Hz, 1H, H5), 5.45 (d, J_{HH} = 3.0 Hz, 1H, H2), 5.27 (d, J_{HH} = 7.2 Hz, 1H, H6), 5.17 (d, J_{HH} = 3.0 Hz, 1H, H3), 2.99 (s, 1H, H8), 2.90 (sept, J_{HH} = 6.6 Hz, 1H, CH of ^{i}Pr), 1.85 (s, 3H, Me of guaiazulene), 1.35 (s, 3H, Me of guaiazulene), 1.35 (d, J_m = 6.6 Hz, 3H, Me of ^{i}Pr), 1.34 (J_{HH} = 6.6 Hz, 3H, Me of ^{i}Pr), 1.14 (s, 9H, ^{t}Bu), 0.89 (s, 9H, ^{t}Bu). ^{13}C{^{1}H}-NMR (C_6D_6, rt): δ 212.5 (CO), 211.2 (CO), 195,4 (CO), 129.9 (C5), 111.0 (C6), 85.3 (C2), 79.6 (C3), 57.2 (C of ^{t}Bu), 36.3 (CH of ^{i}Pr), 30.2 (Me of ^{t}Bu), 29.8 (Me of ^{t}Bu), 22.8 (Me of guaiazulene), 22.1 (Me of ^{i}Pr), 21.8 (Me of ^{i}Pr), 15.8 (C8), 11.6 (Me of guaiazulene). Minor isomer: ^{1}H-NMR(C_6D_6, rt): δ 5.19 (d, J_{HH} = 0.6, 7.8 Hz, 1H, H5), 5.40 (d, J_{HH} = 3.0 Hz, 1H, H2), 5.06 (d, J_{HH} = 7.8 Hz, 1H, H6), 5.14 (d, J_{HH} = 3.0 Hz, 1H, H3), 3.13 (s, IH, H8), 2.93 (sept, J_{HH} = 6.6 Hz, 1H, CH of ^{i}Pr), 1.59 (d, J_{HH} = 0.6 Hz, 3H, Me of guaiazulene), 1.13 (s, 3H, Me of guaiazulene), 1.45 (d, J_{HH} = 12 Hz, 3H, Me of ^{i}Pr), 1.41 (J_{HH} = 7.2 Hz, 3H, Me of ^{i}Pr), 0.92 (s, 9H, ^{t}Bu), 0.79 (s, 9H, ^{t}Bu). ^{13}C{^{1}H}-NMR (C_6D_6, rt): δ 212.3 (CO), 211.0 (CO), 195.5 (CO), 128 (C5), 109.2 (C6), 85.6 (C2), 78.5 (C3), 57.0 (C of ^{t}Bu), 36.3 (CH of ^{i}Pr), 30.2 (Me of ^{t}Bu), 29.8 (Me of ^{t}Bu), 22.8 (Me of guaiazulene), 22.1 (Me of ^{i}Pr), 21.8 (Me of ^{i}Pr), 18.2 (C8), 11.6 (Me of guaiazulene). The ^{13}C resonance due to the C5 carbon (at δ 128) of the minor product was overlapped with the solvent peak (C_6D_6); this was confirmed by ^{1}H–^{13}C HMQC spectrum.

4.3. Thermal and photochemical haptotropic isomerization of *4d–4f*

4.3.1. Thermal interconversion

In a typical example, **4e-A** (5.3 mg, 0.0081 mmol) dissolved in toluene-d_8 (0.4 ml) was placed in a 5 mmϕ NMR tube, and the tube was sealed in a vacuum. The solution was heated to 60 °C in the dark. The ratios of the haptotropic isomers **4e-A** and **4e-B** were periodically measured (every 2 h) by ^{1}H-NMR on the basis of residual proton signals of toluene-d_8 as the internal standard to adjust the integral values. After 10 h, the

Table 6
Crystallographic data for **4d-A** and **5d**

	4d-A	**5d**
Formula	$C_{24}H_{37}NO_4Ru_2$	$C_{25}H_{27}NO_3Ru_2$
Fw	595.61	623.62
Habit	yellow prism	orange prism
Crystal dimensions (mm)	$0.20\times0.10\times0.10$	$0.25\times0.25\times0.40$
Crystal system	monoclinic	triclinic
Space group	$P2_1/c$	$P\bar{1}$
a (Å)	15.113(1)	9.5705(9)
b (Å)	9.5404(7)	15.684(1)
c (Å)	17.175(2)	9.4941(7)
α (°)		106.293(5)
β (°)	94.996(2)	106.604(3)
γ (°)		80.392(2)
V (Å^3)	2467.0(3)	1305.0(2)
Z	4	2
D_{calc} (g cm^{-3})	1.604	1.587
Diffractometer	RAXIS-RAPID (Rigaku)	RAXIS-RAPID (Rigaku)
Radiation (λ, Å)	Mo–K_α (0.71069)	Mo–K_α (0.71069)
Monochromator	graphite	graphite
Temp., (K)	223(2)	296(2)
μ_{calc} (cm^{-1})	12.52	11.90
Abs. Collection	empirical	empirical
θRange (°)	$2.38<\theta<27.48$	$1.36<\theta<27.48$
Reflections collected	5560	5708
Reflections observed	3220 ($>2\sigma$)	5173 ($>2\sigma$)
Number of parameters	280	299
Refinement method	full-matrix least-squares on F^2	full-matrix least-squares on F^2
GOF	0.980	1.123
R_1/wR_2 ($I>2\sigma$(I))	0.0599/0.1186	0.0317/0.0783
R_1/wR_2 (all)	0.1226/0.1400	0.0375/0.0914
$\Delta\rho$ max, (e A^{-3})	0.754 and −0.729	1.004 and −0,815

ratio of **4e-A** to **4e-B** reached 48:52. Further heating of the solution for 33 h resulted in no change of the isomer ratio and no decomposition of the compounds. In the cases of **4d** and **4f**, the isomer ratios in the thermal equilibrium were **4d-A**:**4d-B** = 52:48; **4f-A**:**4f-B** = 50:50.

4.3.2. Photo-induced interconversion

The **4e-A** in toluene-d_8 placed in a NMR tube as described above was subjected to photoirradiation at −20 °C. It was confirmed that no thermal isomerization of **4-A** occurred at this temperature for 18 h while monitoring the ^{1}H-NMR spectra in the dark. After 8 h, the ratio of **4e-A** to **4e-B** reached the photostatic state; the ratio between them was 50:50. Upon irradiation of **4d-A** for 4 h or **4f-A** for 13 h (**4f**), the ratio reached 51:49 or 54:46. In all cases, some amounts of byproducts (14–20%) were observed. Irradiation for 20 h did not change the isomer ratio but was accompanied by extensive decomposition of 50–70% of the compounds.

4.4. X-ray data collection and reduction

Crystallographic data of both **4d-A** and **5d** are summarized in Table 6. Single crystals of **4d-A** and **5d** were grown from a dichloromethane–hexane solution at −30 °C. Data were collected using a Rigaku RAXIS RAPID imaging plate diffractometer with graphite monochromated Mo–K_α radiation ($\lambda = 0.71069$ Å). All data of **4d-A** were collected at 223(2) K, whereas those of **5d** were done at 296(2) K. Data collection was carried out using the program system 'MSC/AFC Diffractometer Control' on a Pentium computer. The absorption collection was carried out empirically. The structures were solved by Patterson method (DIRDIF94 PATTY) [16a] and were refined using full-matrix least-squares (SHELXL-97) [16b] based on F^2 of all independent reflections measured. All non-hydrogen atoms were refined with anisotropic displacement parameters. All H atoms were located at ideal positions and were included in the refinement, but were restricted to riding on the atom to which they were bonded. Isotopic thermal factors of H atoms were held to 1.2–1.5 times (for methyl groups) U_{eq} of the parent atoms.

5. Supplementary information

Crystallographic data (excluding structure factors) for structures reported in this paper have been deposited with the Cambridge Crystallographic Data Center as supplementary publication no. CCDC-167041 for **5d**, and CCDC-167042 for **4a-A**. Copies of the data can be obtained, free of charge, on application to CCDC, 12 Union Road, Cambridge CB2 1EZ, UK (Fax: +44-1223-336033 or e-mail: deposit@ccdc.cam.ac.uk).

Acknowledgements

A part of this study was financially supported by the Japan Society for the Promotion of Science (Grants-In-Aid for Scientific Research 10450343, 12750768, 13450374).

References

[1] (a) For reviews; (a) B.E. Mann, in Comprehensive Organometallic Chemistry; G. Wilkinson, EG.A. Stone, E.W. Abel, (Eds.) Pergamon, Oxford; Vol. 3 (1982) Chap. 20;
(b) B.E. Mann, Chem. Soc. Rev. 15 (1986) 167;
(c) X.A. Albright, P. Hofmann, R. Hoffmann, C.P. Lillya, P.A. Dobosh, J. Am. Chem. Soc. 105 (1983) 3396;
(d) G. Degenello, Transition Metal Complexes of Cyclic Polyolefines; Academic Press; London (1982).

[2] (a) Representative examples of the haptotropic rearrangement of mononuclear transition metal complexes; (a) P. M, Treichel, J.W. Johnson, Inorg. Chem. 16 (1977) 749;
(b) R.U. Kriss, P.M. Treichel, J. Am. Chem. Soc. 108 (1986) 853;
(c) M.E. Rerek, F. Basolo, Organometallics 3 (1984) 647;
(d) K. Nakasuji, M. Yamaguchi, I. Murata, J. Am. Chem. Soc. 108 (1986) 325;
(e) O.I. Trifonova, E.A. Ochertyanova, N, G. Akhmedov, V.A. Roznyatovsky, D. N, Laikov, N.A. Ustynyuk, Y.K. Ustynyuk, Inorg. Chim. Acta 280 (1998) 328;
(f) Y.F. Oprunenko, N.G. Akhmedov, D, N. Laikov, S.G. Malyugina, V.I. Mstislavsky, V.A. Roznyatovsky, Y.A. Ustynyuk, N.A. Ustynyuk, J. Organomet. Chem. 583 (1999) 328;
(g) L.F. Veiros, J. Organomet. Chem. 587 (1999) 221.

[3] (a) J. O'Connor, C.P. Casey, Chem. Rev. 87 (1987) 307;
(b) J.P. Collman, L.S. Hegedus, J.R. Norton, R.G. Finke, Principles and Applications of Organotransition Metal Chemistry, University Science Books, 1987.

[4] (a) E.A. Cotton, D.L. Hunter, P. Lahuerta, Inorg. Chem. 14 (1975) 511;
(b) M.R. Churchill, J. Wormald, Inorg. Chem. 9 (1970) 2239;
(c) F.A. Cotton, B.E. Hanson, J.R. Kolb, P. Lahuerta, G.G. Stanley, B.R. Stults, A.J. White, J. Am. Chem. Soc. 99 (1977) 3673;
(d) H. Nagashima, A. Suzuki, The Reports of Inst. Adv. Material Study, Kyushu Univ. 11 (1997) 175.

[5] (a) H. Nagashima, T. Fukahori, K. Itoh, J. Chem. Soc. Chem. Commun. (1991) 786;
(b) H. Nagashima, T. Fukahori, M. Nobata, A. Suzuki, M. Nakazawa, K. Itoh, Organometallics 13 (1994) 3427;
(c) K. Matsubara, T. Oda, H. Nagashima, Organometallics 20 (2001) 881.

[6] Y. Yamamoto, Coord. Chem. Rev. 32 (1980) 193, and references cited therein.

[7] (a) Involvement of η^1-allyl intermediates in the substitution reactions of η^3-allyl complexes; (a) G. Sbrana, G. Braca, E. Benedetti, J. Chem. Soc. Dalton Trans. (1975) 754;
(b) C.F.J. Barnard, J.A. Daniels, P.R. Holland, R.J. Mawby, J. Chem. Soc. Dalton Trans. (1980) 2418;
(c) H. Lehmkuhl, H. Mauermann, R. Benn, Liebigs Ann. Chem. (1980) 754.

[8] Conversion of η^3- to η^1-allyl coordination mode of ruthenium complexes; H. Nagashima, K. Mukai, Y. Shiota, K. Yamaguchi, K. Ara, T. Fukahori, H. Suzuki, M. Akita, Y. Moro-oka, K. Itoh, Organometallics 9 (1990) 799.

[9] Two isomers of **6d** (the isomer ratio = 60:40) were assigned from the following spectroscopic features: (1) characteristic high field shift of H and C resonances of H8 and C8 (δ 2.99, 3.13 in ^{1}H-NMR, δ_C 15.8, 18.2 in ^{13}C-NMR); (2) two sets of four ^{13}C resonances due to the coordinated CO ligands at 6 213.3, 212.5, 211.2,195.4 and 212.3, 211.0, 197.8, 195.5; (3) two IR absorptions (ν_{C-N}) at 2182 and 2156 cm^{-1}.

[10] We were interested in thermolysis of **6d** at 80 °C, which might afford diisocyanide derivatives of **1**, (μ_2,η^3:η^5-guaiazulene)$Ru_2(CO)_3(CN^tBu)_2$. The desired product was identified by spectroscopy, however, attempted isolation was unsuccessful. The compound was completely decomposed during column chromatography (silica or alumina), whereas fractional recrystallization was unsuccessful because of high solubility in the common organic solvents.

[11] (a) For example; (a) M.I. Bruce, J.G. Malisons, R.C. Wallis, J.M. Patrick, B.W. Skelton, A. H, White, J. Chem. Soc. Dalton Trans. (1983) 2365;
(b) L.J. Farrugia, C. Rosenhahn, S. Whitworth, J. Cluster Sci. 9 (1998) 505;
(c) A.A. Chalmers, D.C. Liles, E. Meintjies, H.E. Oosthuizen, J.A. Pretorius, E. Singleton, Chem. Commun. (1985) 1340;
(d) M.O. Albers, D.C. Liles, E. Singleton, J.E. Stead, M.M. de V. Steyn, Organometallics 5 (1986) 1262;
(e) M.O. Albers, D.C. Liles, E. Singleton, J.E. Stead, M.M. de V. Steyn, Organometallics 5 (1986) 1262;
(f) F.M. Conroy-Lewis, S.J. Simpson, L. Brammer, A.G. Orpen, J. Organomet. Chem. 406 (1991) 197.

[12] (a) Site exchange processes of CO ligands in several dinuclear complexes having bridging polyene and polyenyl ligands; (a) Ref. [4a];
(b) F.A. Cotton, B.E. Hanson, J.R. Kolb, P. Lahuerta, Inorg. Chem. 16 (1977) 89;
(c) F.A. Cotton, B.E. Hanson, J.R Kolb, P. Lahuerta, G.G. Stanley, B.R. Stults, A.J. White, J. Am. Chem. Soc. 99 (1977) 3673.

[13] For a review including site exchange processes of isonitrile ligands; E. Singleton, H. E, Oosthuizen, Adv. Organomet. Chem. 22 (1983) 209.

[14] Conville and coworkers discussed the arrangement of the ligands with $Mn_2(CO)_9(PR_3)$ and $Re_2(CO)_9(CNR)$. They concluded that the electron-donating CNR or PR_3 ligand was favorably coordinated at *trans*-position of the good π-acceptor, namely, the CO ligand. However, sterically more bulky PR_3 caused significant repulsion with the CO ligand bound to the adjacent metal center, and, therefore, the PR_3 ligand in $Mn_2(CO)_9(PR_3)$ is located at the *trans*-position of the $Mn(CO)_5$ moiety. G.W. Harris, J.C.A. Boeyens, N.J. Conville, Organometallics 4 (1985) 914.

[15] I. Ugi, R. Meyer, Organic Synthesis, vol. Collect V, Wiley, New York, 1973, p. 1060.

[16] (a) The DIRDIF-94 program system, Technical Report of the Crystallography Laboratory, University of Nijmegen, The Netherlands. R.T. Beurskens, G. Admiraal, G. Beurskens, W.R Bosman, R. de Gelder, R. Israel, and J.M.M. Smits, 1994;
(b) G.M. Sheldrick, SHELXL-97, 1997.